Progress In Electromagnetics Research Letters, Vol. 113, 1–6, 2023

Modeling and Design of CPW Spoof Surface Plasmon Polariton with Reduced Transversal Width

Rui-Feng Cao and Lin Li*

Abstract—In this paper, equivalent circuit models are first presented for characterizing CPW SSPPs with etched slot. The asymptotic frequency and dispersion are investigated based on the theoretical model. And the analyses reveal that both the asymptotic frequency and dispersion curve can be manipulated by changing the inductance brought by the etched slots and the capacitance of the loaded capacitors. To validate the propagation performance, the proposed SSPP structure was fabricated and tested. The experimental results are consistent with the theoretical analysis, indicating that the designed SSPP structure possesses excellent low-pass filtering characteristics. Compared with traditional SSPP structures, the proposed structure exhibits a much narrower transversal width and does not require mode-conversion structures.

1. INTRODUCTION

Surface plasmon polaritons (SPPs) refer to surface electromagnetic waves that propagate along the interface of a metal and dielectric, but decline sharply in the direction perpendicular to the interface [1]. In the past few years, SPPs have been widely referenced in the optical field because of their distinctive characteristics of confining the field near the surface [1]. However, due to the limitation of the dielectric constant of metals, SPPs do not exist in the microwave and THz bands [1]. Recently, various structures that support SSP modes in the microwave and THz bands have been reported [2–4]. However, for most of these reported SSPPs, relatively complicated mode-conversion structures such as flaring ground are required to convert guided waves to SSPP wave, which increase transversal width largely.

In [5], a new CPW SSPP waveguide is proposed with a simple and efficient mode conversion transition structure. Based on the proposed SSPP in [5], many new SSPPs are presented. In [6], an SSPP waveguide loaded with two half-wavelength slot resonators on both sides was proposed, exhibiting excellent low-pass characteristics. In [7], a capacitor-loaded T-shaped CPW SSPP with a small groove depth was proposed. However, to the best of our knowledge, the equivalent model for such CPW SSPPs has not been reported so far, which limits the application of such SSPPs largely.

In this paper, for the first time, an equivalent circuit model is established to describe the characteristics of the CPW SSPPs in [5–7]. The investigation of the CPW SSPPs based on equivalent circuit model reveals that the dispersion curves can be easily controlled by changing the inductance brought by the etched slots and the capacitance of the loaded capacitors. According to the method derived from the model analyses, a CPW-based SSPP structure is designed, which can effectively reduce the transversal width.

2. THEORY AND DESIGN PRINCIPLE

Figure 1 illustrates the SSPP unit cell proposed in this paper. The coplanar waveguide (CPW) line has a line width of w_m, a coupled gap of w_p, and a period of p. To excite the SSPP waves, two spiral-shaped

Received 12 June 2023, Accepted 18 September 2023, Scheduled 8 October 2023
* Corresponding author: Lin Li (lilin_door@hotmail.com).
The authors are with the School of Information Science and Engineering, Zhejiang Sci-Tech University, Hangzhou, Zhejiang, China.

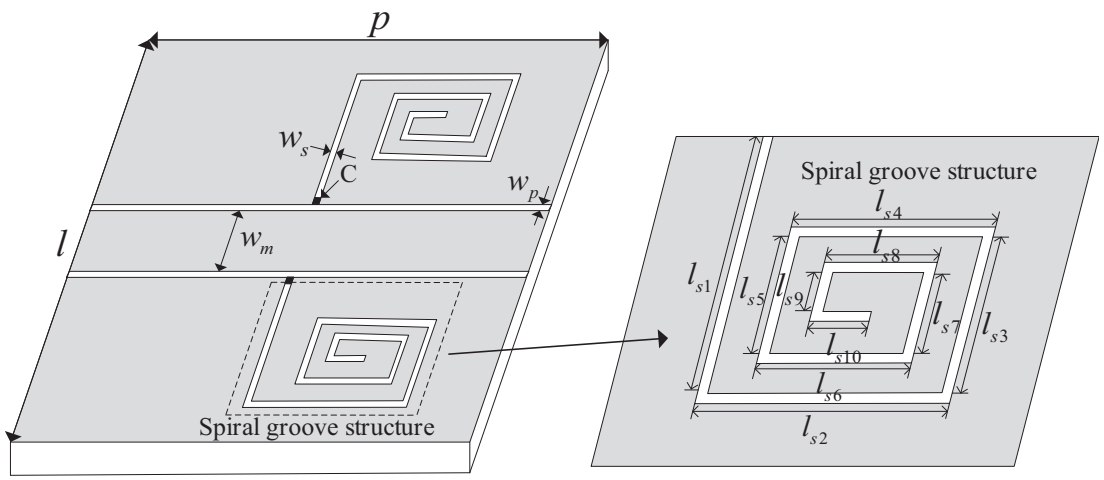

Figure 1. Schematic diagram of the proposed SSPP unit cell.

groove structures with the width of w_e are etched on both sides of the CPW grounds. Two extra capacitors are loaded on the etched grooves to further manipulate the dispersion curves. The substrate in Figure 1 and all the following examples in this paper is FR4 with a thickness of 0.8 mm, a dielectric constant of 4.4, and a loss tangent of 0.02.

For the periodic structure, its electromagnetic (EM) characteristics can be described by its unit cell. And its dispersion curve can be drawn from the scattering matrix calculated from the circuit model of the cell. In order to offer the general understanding of the periodical SSPP structure in Figure 1, the equivalent circuit model in Figure 2 is proposed by using hybrid distributed and lumped circuit elements. As shown in Figure 2, the CPW lines are represented by the transmission lines (TLs) with impedance Z_1 and electrical length θ_1. The two spiral grooves are modeled by the two inductors of L in Figure 2. The two transformers in Figure 2 depict the electromagnetic coupling between the CPW lines and spiral-shaped groove structures. The two C represent the loaded capacitors on the slots. The impedance Z_L represents the impedance of the parallel circuit composed of L and C.

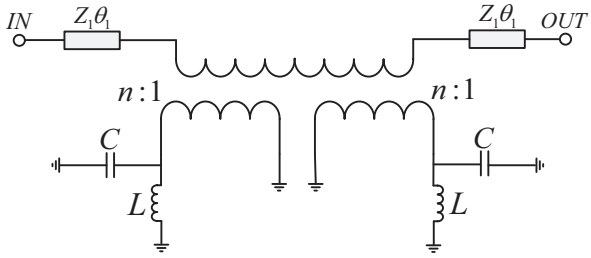

Figure 2. The equivalent circuit model of a unit cell.

In the equivalent circuit model, current and voltage are defined as the current flowing through a conductor and the potential difference between the conductor and infinity, respectively. For the periodic structures, the following relation between input (V_n, I_n) and output (V_{n+1}, I_{n+1}), i.e., voltages and currents of the unit cell, can be calculated.

$$V_{n+1} = V_n e^{j\beta p}, \quad I_{n+1} = I_n e^{j\beta p} \tag{1}$$

where β is propagation constants.

The transmission matrix, which is called $ABCD$ matrix, can also be used to describe the input-output relationships between adjacent cells in periodic structures.

$$\begin{bmatrix} V_{n+1} \\ I_{n+1} \end{bmatrix} = \begin{bmatrix} A & B \\ C & D \end{bmatrix} \begin{bmatrix} V_n \\ I_n \end{bmatrix} \tag{2}$$

By utilizing the circuit parameters of the proposed equivalent circuit model, the $ABCD$ matrix can be computed as follows

$$\begin{bmatrix} A & B \\ C & D \end{bmatrix} = \begin{bmatrix} \cos^2\theta_1 + \dfrac{jZ_L \sin\theta_1 \cos\theta_1}{Z_1 n^2} - \sin^2\theta_1 & jZ_1 \sin\theta_1 \cos\theta_1 + \dfrac{\cos^2\theta_1 Z_L}{n^2} + jZ_1 \sin\theta_1 \cos\theta_1 \\ \dfrac{j\sin\theta_1 \cos\theta_1}{Z_1} - \dfrac{\sin^2\theta_1 Z_L}{n^2 Z_1^2} + \dfrac{j\sin\theta_1 \cos\theta_1}{Z_1} & \cos^2\theta_1 + \dfrac{jZ_L \sin\theta_1 \cos\theta_1}{Z_1 n^2} - \sin^2\theta_1 \end{bmatrix} \tag{3}$$

The impedance ZL can be calculated according to the following equation.

$$Z_L = \frac{jwL}{1 - w^2 CL} \tag{4}$$

Since the proposed structure in this paper is a symmetry structure, the propagation constants can be calculated from formula (5).

$$\cos(\beta p) = A \tag{5}$$

Based on the formula presented above, the correlation between the asymptotic frequency f_a and circuit components can be derived as below.

$$4\pi^2 n^2 CL f_a^2 - 2\pi L \cot\theta_1 f_a - Z_1 n^2 = 0 \tag{6}$$

As shown in Equation (6), the values of capacitor C and inductor L exert influence on the asymptotic frequency f_a. Figures 3(a) and 3(b) illustrate the curves of calculated f_a from (6) with different C and L, respectively. It can be observed from the two figures that the larger the values of L or C is, the smaller the asymptotic frequency f_a is.

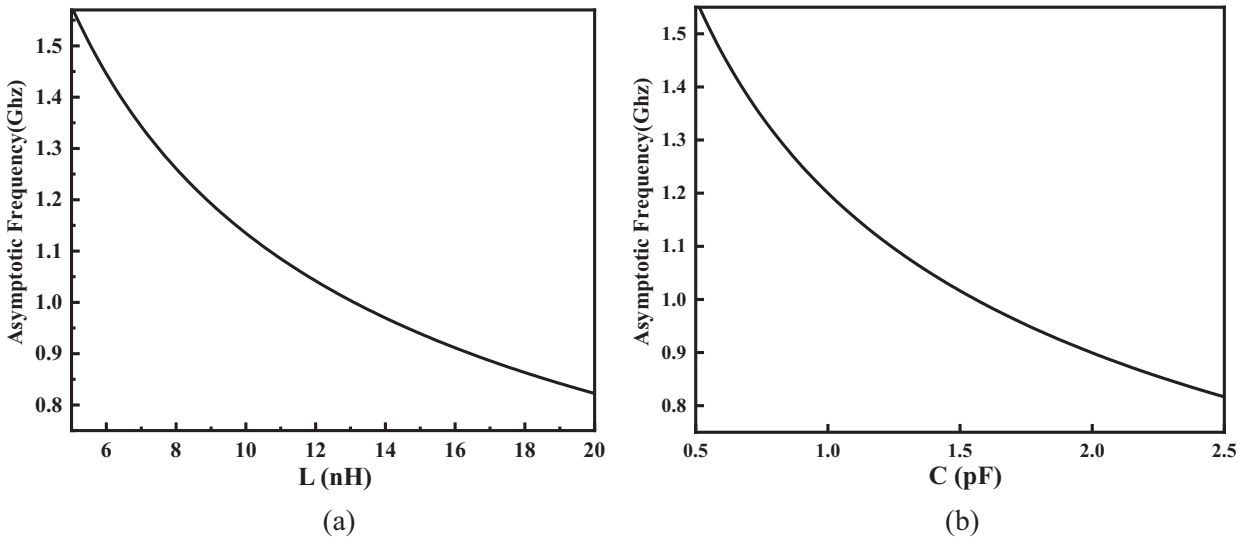

Figure 3. (a) Calculated f_a with different L. (b) Calculated with f_a different C. ($w_m = 2$, $w_p = 0.2$, $w_s = 0.2$, $p = 10$, $l = 15$, $h = 0.8$, $l_{s1} = 3$, $l_{s2} = 6.8$, $l_{s3} = 2.5$, $l_{s4} = 6$, $l_{s5} = 1.7$, $l_{s6} = 5.2$, $l_{s7} = 1.1$, $l_{s8} = 4.3$, $l_{s9} = 0.5$, $l_{s10} = 3.5$ unit: mm).

Generally, the smaller the asymptotic frequency is, the more apparent the dispersion curve deviates from light line. To further verify the above conclusion, Figure 4(a) compares the circuit and EM simulated dispersion with different C. Good agreement between the two methods demonstrates the accuracy of the proposed equivalent circuit model. A revealed in the above discussion, the larger the value of C is, the more obvious the SSPP response is.

Another method to manipulate the dispersion curve is to change L, which can be realized by changing the number of turns in the spiral grooves. Dispersion curves of three different spiral grooves are given in Figure 4. The inductance of the three spiral grooves is 10.4 nh, 8.7 nh, and 2.9 nh, respectively.

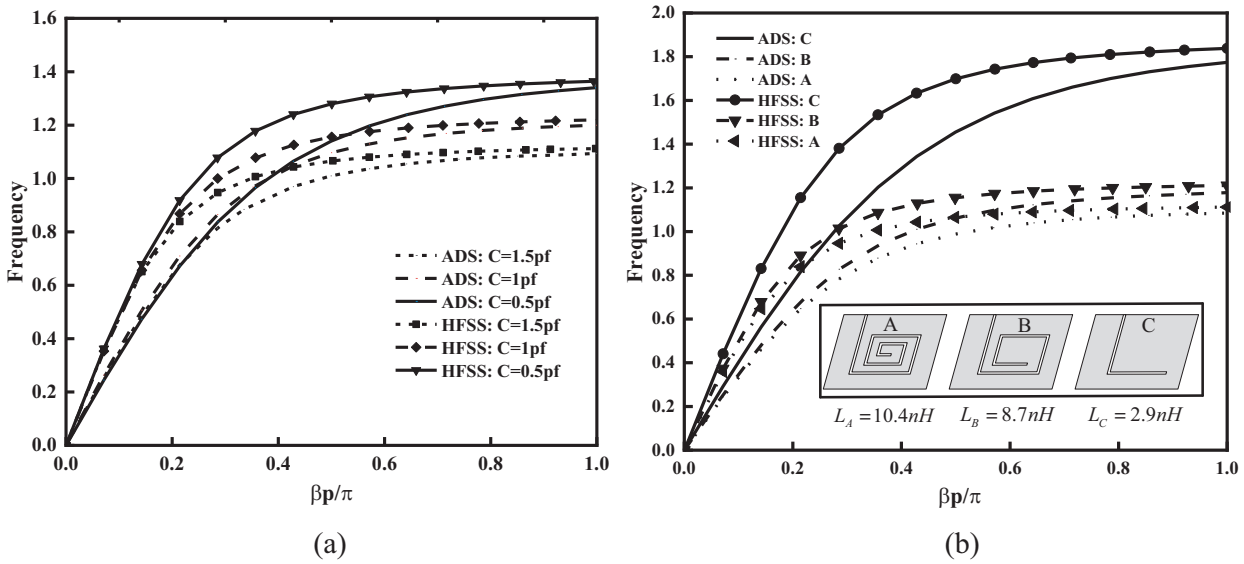

Figure 4. Dispersion curves. (a) Different capacitance values. (b) Spiral grooves with different numbers of turns. ($w_m = 2$, $w_p = 0.2$, $w_s = 0.2$, $p = 10$, $l = 15$, $h = 0.8$, $l_{s1} = 3$, $l_{s2} = 6.8$, $l_{s3} = 2.5$, $l_{s4} = 6$, $l_{s5} = 1.7$, $l_{s6} = 5.2$, $l_{s7} = 1.1$, $l_{s8} = 4.3$, $l_{s9} = 0.5$, $l_{s10} = 3.5$ unit: mm).

The consistency between the results and the conclusion drawn from Figure 3 in the previous section validates the accuracy of the proposed model. As seen in the graph, the greater the number of turns in the spiral grooves is, the higher the value of equivalent inductance is, and the more obvious the SSPP response is.

Based on the above analyses, SSPPs with reduced transversal width can be easily realized by increasing the inductance of the spiral grooves and the capacitance of the loaded capacitors.

3. DESIGN AND MEASUREMENT

According to the dispersion characteristics of the unit cell depicted in Figure 1, an SSPP TL with low-pass filtering characteristics is presented. As shown in Figure 5, the schematic configurations of the

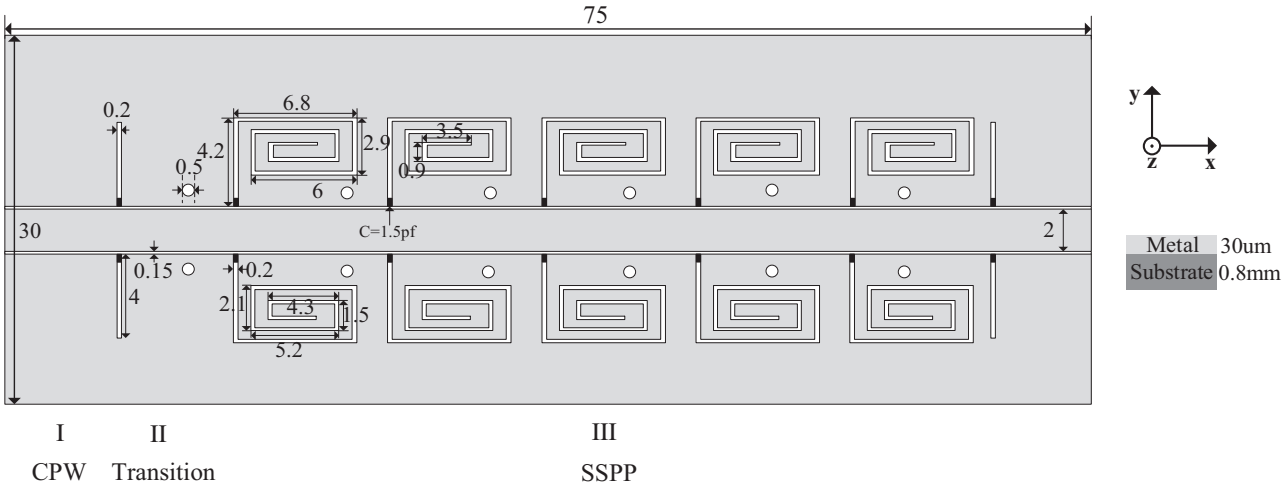

Figure 5. The schematic configurations of the SSPP waveguide.

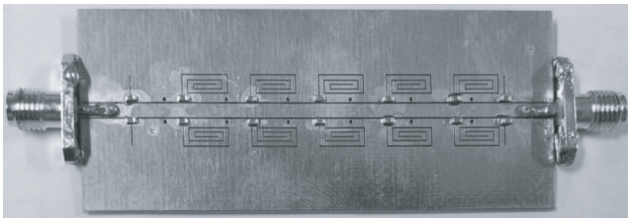

Figure 6. Fabricated prototype of the SSPP waveguide.

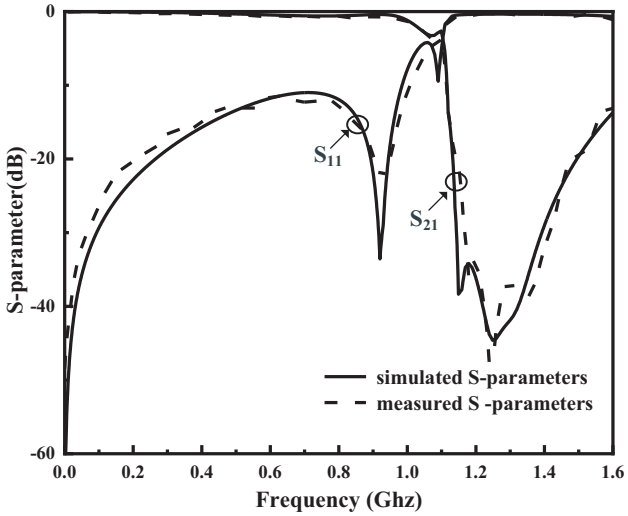

Figure 7. Simulated and measured S-parameters.

proposed SSPP TL consists of three parts: CPWs serving as input/output ports for easy measurement, a transition region established between CPWs and SSPP for stable signal transmission, and five periodic capacitor-loaded SSPP units. A photograph of the fabricated SSPP is shown in Figure 6.

Figure 7 depicts the S-parameters obtained from both simulation and measurement, showing a remarkable consistency between the two results. This indicates that the SSPP TL designed in this study exhibits excellent filtering characteristics consistent with the theoretical design, while occupying a relatively small volume. The slight discrepancy between the simulation and testing results may be attributed to the tolerances introduced by printed circuit board fabrication and capacitors, as well as differences in the measurement environment.

Table 1 compares the SSPP structure proposed in this paper with some reported SSPPs in terms of the asymptotic frequency f_a, groove shape, capacitance-load, and transversal width w_t. Obviously, the SSPP proposed in this paper has the narrowest transverse width and does not require mode-conversion structures. Moreover, by increasing the number of spiral groove turns and the capacitance of the loaded capacitors, the transverse width can be further reduced.

Table 1. Performance of previous works and this word.

Ref.	f_a (Ghz)	Shape	Mode conversion	w_t (λ_a)
[5]	8.9	Spiral	Not required	0.047
[6]	4.8	Spiral	Not required	0.061
[7]-A	1.78	Strip	Not required	0.053
[7]-B	1.78	T-shape	Not required	0.035
[8]	5.8	Strip	Required	0.058
[9]	8.1	Strip	Required	0.081
This work	1.1	spiral	Not required	0.015

λ_a: the wavelength at f_a.

4. CONCLUSION

This paper introduces a capacitor-loaded SSPP structure based on CPW and its equivalent circuit model. Theoretical and experimental verifications suggest that this structure exhibits low asymptotic frequency and low pass filtering characteristics, thus advancing miniaturization of plasma devices.

REFERENCES

1. Barnes, W. L., A. Dereux, and T. W. Ebbesen, "Surface plasmon subwavelength optics," *Nature*, Vol. 424, 824–830, Aug. 2003.
2. Gao, X. and T. J. Cui, "Spoof surface plasmon polaritons supported by ultrathin corrugated metal strip and their applications," *Nanotechnol. Rev.*, Vol. 4, No. 3, 239–258, 2015.
3. Kianinejad, A., Z. N. Chen, and C.-W. Qiu, "Design and modeling of spoof surface plasmon modes-based microwave slow-wave transmission line," *IEEE Trans. Microw. Theory Tech.*, Vol. 63, No. 6, 1817–1825, 2015.
4. Shen, S., B. Xue, M. Yu, and J. Xu, "A novel three-dimensional integratedspoof surface plasmon polaritons transmission line," *IEEE Access*, Vol. 7, 26900–26908, 2019.
5. Li, J., J. Shi, K.-D. Xu, Y.-J. Guo, A. Zhang, and Q. Chen, "Spoof surface plasmon polaritons developed from coplanar waveguides in microwave frequencies," *IEEE Photonics Technol. Lett.*, Vol. 32, No. 22, 1431–1434, 2020.
6. Li, J., K.-D. Xu, J. Shi, Y.-J. Guo, and A. Zhang, "Spoof surface plasmon polariton waveguide with switchable notched band," *IEEE Photonics Technol. Lett.*, Vol. 33, No. 20, 1147–1150, 2021.
7. Wang, C.-M., W.-Q. Xu, L. Li, H. Liu, and Y. Kuang, "Capacitor-loaded coplanar waveguide spoof surface plasmon polariton with reduced transversal width," *IEEE Photonics Technol. Lett.*, Vol. 35, No. 10, 557–560, 2023.
8. Tang, X.-L., Q. Zhang, S. Hu, A. Kandwal, T. Guo, and Y. Chen, "Capacitor-loaded spoof surface plasmon for flexible dispersion control high-selectivity filtering," *IEEE Microw. Wirel. Compon. Lett.*, Vol. 27, No. 9, 806–808, 2017.
9. Shi, Z., Y. Shen, and S. Hu, "Spoof surface plasmon polariton transmission line with reduced line-width and enhanced field confinement," *Int. J. RF Microw. Comput-Aid. Eng.*, Vol. 30, No. 8, e22276, 2020.